ISSN 1068-3739, Russian Meteorology and Hydrology, 2021, Vol. 46, No. 4, pp. 269–279. Allerton Press, Inc., 2021.
Russian Text The Author(s), 2021, published in Meteorologiya i Gidrologiya, 2021, No. 4, pp. 86–100.

Retrieval of Volcanic Ash Parameters from Satellite Data

A. A. Filei[a]* and F. Marenco[b]

[a]*Far Eastern Center, Planeta Research Center for Space Hydrometeorology, ul. Lenina 18, Khabarovsk, 680000 Russia*

[b]*Met Office, FitzRoy Road, Exeter, Devon, EX13PB United Kingdom*

**e-mail: vmer@dvrcpod.ru*

Received May 19, 2020
Revised May 28, 2020
Accepted June 25, 2020

Abstract—A method for retrieving volcanic ash parameters from satellite data is presented. The fundamental difference between the presented methodology and classical algorithms for the retrieval of volcanic ash parameters is the simultaneous use of various optical models of volcanic clouds. The models contain information not only about volcanic rocks (andesite or basalt) but also about their combinations with water drops and the aqueous solution of sulfuric acid. The volcanic ash parameters are determined by the characteristics of solar radiation reflected from a volcanic cloud and the cloud's self-radiation in the infrared atmospheric window. The volcanic ash parameters are retrieved according to the Meteosat-9 SEVIRI satellite radiometer for the case of the Eyjafjallajokull volcano eruption (Iceland, May 2010). The results are compared with data of aircraft lidar measurements and show a good qualitative and quantitative agreement.

DOI: 10.3103/S1068373921040087

Keywords: Volcanic ash, mass concentration, volumetric extinction coefficient, optical depth, effective radius, satellite data

INTRODUCTION

Volcanic eruptions can cause various regional and global consequences, starting from the destruction of infrastructure and ecosystem near a volcano [25] and ending with the impact on global climate [16]. In addition, volcanic ash clouds crossing aviation routes can pose a serious threat to the flight safety. For example, the recent major eruptions of the Icelandic volcanoes in 2010 and 2011 led to the air traffic disruption in Europe and caused losses of billions of dollars for airlines [17]. In view of this, there has been a need in the timely detection of volcanic ash released to the atmosphere during eruptions and in the organization of routine monitoring of volcanic cloud propagation with simultaneous determination of concentration and microphysical parameters of ash particles.

Most techniques for the calculation of volcanic ash parameters from satellite data are based on the analysis of outgoing infrared radiation in the spectral range of 10–12 m, on so called reverse absorption technique based on the "split transparency window" [27]. Following this approach, it is possible to calculate its parameters for certain atmospheric conditions using an optical model of volcanic ash if the outgoing infrared radiation measured in the satellite instrument channels is known. However, there are great differences [28] in the estimates of retrieved parameters determined by different methods based on data of the same satellite instruments. The factors causing these discrepancies are well known and were discussed in many papers [7, 21, 24, 27].

One of the main factors affecting the accuracy of determination of volcanic ash parameters is the choice of an optical model. The difference of the presented method for retrieving volcanic ash parameters from classic schemes, when the choice comes to two optical ash models (andesite or basalt), consists in the simultaneous use of several models of volcanic clouds composed of the ash of different nature in combination with water drops or the aqueous solution of sulfuric acid (H_2SO_4). The ash parameters are determined by the characteristics of both solar radiation reflected from the volcanic cloud and cloud's self-radiation in

infrared atmospheric transparency windows (in the area of 10 m). Taking into account the diversity of observation geometry and variability of optical atmospheric conditions, the radiation calculations in solar and infrared regions are used to determine the signals in the spectral channels of satellite scanners for each volcanic cloud model and the series of values of optical depth ($_{aer}$) and effective radius (r_{ef}). Such signals are reflection coefficients in the solar spectral range and the values of brightness temperature in the infrared region. The calculated signals of all models for a particular observation scheme are compared with the real ones, i.e., with the signals determined directly from measurements in the satellite instrument channels. The technique for minimizing the root-mean-square residual between the calculated and measured signals is used to choose a particular model; then, the volcanic ash parameters are estimated.

The cases of eruptions of the Eyjafjallajokull volcano (Iceland) in May 2010 were analyzed to validate the satellite estimates of volcanic ash parameters, including $_{aer}$, r_{ef}, and mass concentration (M_{aer}). The ash parameters were evaluated using Meteosat-9 SEVIRI multichannel scanner measurement data (https://www.wmo-sat.info/oscar/instruments/view/503). Measurement data obtained during the experimental flight of FAAM BAe-146 research aircraft were used as reference ones.

SIMULATION OF SATELLITE SIGNALS OVER VOLCANIC CLOUDS

When modeling signals in infrared channels of the satellite instrument, it was assumed that the volcanic cloud is a homogeneous flat slab. Then, the intensity of infrared radiation R_{obs} registered by the satellite instrument at the atmosphere top is defined by the following expression [20]:

$$R_{obs} \quad (1 \quad)R_{clr} \quad (R_{ac} \quad t_{ac}B(T_{ef}\ )) \tag{1}$$

where is the coefficient of effective emissivity of the volcanic cloud; R_{clr} is the radiation of the "clear" atmosphere; R_{ac} is the atmospheric radiation over the volcanic cloud; t_{ac} is the coefficient of atmospheric transmission over the volcanic cloud; B is the Planck's function; T_{ef} is effective temperature of the volcanic cloud.

The parameter T_{ef} in (1) determines temperature of the black body that corresponds to the outgoing radiation from the cloud top. The coefficient is analytically connected with the transmission coefficient:

$$t \quad 1 \quad \exp(\ L \ _{ext}/\cos\ ) \tag{2}$$

where t is the transmission coefficient of the volcanic cloud; L is the geometric thickness of the cloud; $_{ext}$ is the volumetric extinction coefficient; is the zenith viewing angle.

Thus, the coefficient is directly connected with microphysical parameters of the volcanic cloud, which are determined by the coefficient $_{ext}$. There is an obvious relation between $_{ext}$ and optical depth $_{aer}$:

$$_{aer} \quad L \ _{ext} \quad \ln(1 \quad)\cos\ . \tag{3}$$

The ratio of the values of optical depth for the certain pair of infrared channels, for example, at the wavelengths of 12 and 11 m, is usually considered to determine the microphysical structure of the ash cloud. The similar ratio is presented in [18] to determine cirrus cloud parameters, in particular, the effective radius r_{ef} from AVHRR satellite instrument data. The ratio is expressed through the coefficient $_{ef}$ using the following formula:

$$_{ef} \quad \frac{_{aer,12}}{_{aer,11}} \quad \frac{\ln(1 \quad _{12})}{\ln(1 \quad _{11})} \quad \frac{\ln \dfrac{R_{obs,12} \quad (R_{ac,12} \quad t_{ac,12}B(T_{ef,12}))}{R_{clr,12} \quad (R_{ac,12} \quad t_{ac,12}B(T_{ef,12}))}}{\ln \dfrac{R_{obs,11} \quad (R_{ac,11} \quad t_{ac,11}B(T_{ef,11}))}{R_{clr,11} \quad (R_{ac,11} \quad t_{ac,11}B(T_{ef,11}))}}. \tag{4}$$

The coefficient $_{ef}$ depends on the microphysical parameters of volcanic clouds and is the main parameter for estimating these parameters from satellite data.

Several unknown parameters, namely, R_{clr}, R_{ac}, t_{ac}, and T_{ef} should be determined to compute $_{ef}$ from satellite data. The values of R_{clr}, R_{ac}, t_{ac} are determined using the RTTOV fast radiative transfer model (https://www.nwpsaf.eu/site/software/rttov/); the temperature of the underlying surface T_{surf} and the profiles of temperature and water vapor obtained from the GFS numerical weather prediction model with a spatial resolution of 0.25 are used at its input. In addition, the emissivity of the underlying surface obtained at https://cimss.ssec.wisc.edu/iremis/ was additionally used to calculate R_{clr}.

The determination of T_{ef} is especially difficult. For optically dense clouds, T_{ef} is roughly equal to the cloud top temperature T_{cld}. The less optically dense the ash cloud is, the more significant the difference between T_{ef} and T_{cld} is. The radiation from optically thin clouds is formed by underlying atmospheric (cloud) layers and the Earth surface. According to [11], the condition > 0.4 should be met for the precise determination of T_{cld}. In the present paper, T_{cld} is determined by the method from [11].

According to [18, 26], the interpretation of (4) through the optical parameters of aerosol with account of infrared radiation scattering has the following form:

$$_{theo} \quad \frac{(1 \quad _{12} g_{12})\ _{ext,12}}{(1 \quad _{11} g_{11})\ _{ext,11}} \tag{5}$$

where is single-scattering albedo; g is the skewness of the scattering indicatrix.

The coefficient $_{ef}$ determined from satellite measurements of optical depth at 12 and 11 m, according to [18], is equal to the model $_{theo}$ calculated by the Mie theory:

$$_{ef} \quad _{theo}. \tag{6}$$

As shown in [18], comparing $_{ef}$ with $_{theo}$, it is possible to determine the type of aerosol, its particle size distribution, and effective radius r_{ef}, and, with account of the value of $_{aer}$ calculated using (3), to determine the mass concentration using the following formula [9, 22]:

$$M_{aer} \quad W_{aer} L \quad W_{aer} \frac{_{aer,11}}{_{ext,11}} \quad \frac{_{aer,11}}{k_{ext,11}};$$
$$k_{ext,11} \quad \frac{1}{} \frac{\int_{r_1}^{r_2} Q_{ext,11} r^2 n(r) dr}{\frac{4}{3} \int_{r_1}^{r_2} r^3 n(r) dr} \tag{7}$$

where W_{aer} is volume concentration; $Q_{ext,11}$ is extinction efficiency factor; r is particle radius; is the aerosol particle density; $n(r)$ is the particle size distribution function; $k_{ext,11}$ is the mass extinction coefficient.

The parameter $Q_{ext,11}$ is dimensionless, it determines the extinction of electromagnetic radiation due to absorption and scattering and is equal to the ratio of the effective cross-section of the particle extinction $_{ext}$ to the particle area:

$$Q_{ext,11} \quad \frac{_{ext}}{r^2}. \tag{8}$$

Thus, having the optical models of volcanic aerosol and having preliminarily calculated $_{ef}$ and $_{aer}$, it is possible to use satellite data for determining M_{aer} and r_{ef}. The accuracy of the retrieved ash parameters depends on the optimum choice of such model.

OPTICAL MODELS OF VOLCANIC CLOUDS

The application of models for determining the parameters of volcanic ash and any aerosol is generally a common approach to solving such problems in the field of remote sensing. The difficulty of implementing this approach for retrieving the volcanic ash parameters consists in the optimum choice of the model for specific conditions of observations with a satellite instrument. The ash of each volcano has a unique composition and consists of different magmatic rocks: from andesite to andesite-basalt and dacite [1]. Volcanic clouds are a mixture of different components that can be represented by ash, water drops, and H_2SO_4 aqueous solution. Hence, the choice of optical models comes to the selection from different combinations of aerosol components of volcanic clouds. In the present study, the models of dependences of optical parameters k_{ext}, , g on the wavelength were constructed in the form of lookup tables (LUT) for different values of r_{ef} and combinations of volcanic rocks with water drops and H_2SO_4 (the model construction is described in more detail in [4], the full list of optical models can be found at https://www.dvrcpod.ru/ASH.php). Let us consider only separate aerosol fractions of a volcanic cloud.

Table 1 presents the optical and microphysical parameters of aerosol fractions for the unit optical depth ($_{aer,0.55} = 1$). The parameters are given for two wavelengths: 0.55 and 11 m.

Table 1. Optical and microphysical parameters of cloud components for the unit optical depth ($_{\text{aer, 0.55}} = 1$)

Parameter		11 m				0.55 m			
r_{ef}	M_{aer}	$_{\text{aer}}$	k_{ext}		g	$_{\text{aer}}$	k_{ext}		g
				Andesite					
0.5	0.63	0.07	0.14	0.23	0.25	1.0	1.56	0.98	0.71
1.0	1.27	0.17	0.22	0.39	0.38	1.0	0.79	0.97	0.72
2.0	2.82	0.37	0.25	0.47	0.49	1.0	0.35	0.94	0.76
3.0	4.43	0.50	0.22	0.48	0.55	1.0	0.23	0.92	0.79
5.0	7.68	0.61	0.16	0.49	0.63	1.0	0.13	0.88	0.82
7.0	10.95	0.64	0.12	0.50	0.69	1.0	0.09	0.85	0.84
9.0	14.23	0.63	0.09	0.50	0.73	1.0	0.07	0.82	0.85
11.0	17.53	0.62	0.07	0.51	0.76	1.0	0.06	0.80	0.86
				Basalt					
0.5	0.69	0.06	0.12	0.25	0.26	1.0	1.44	0.99	0.68
1.0	1.42	0.16	0.19	0.42	0.39	1.0	0.70	0.98	0.70
2.0	3.16	0.37	0.23	0.48	0.48	1.0	0.32	0.96	0.74
3.0	4.96	0.50	0.20	0.50	0.54	1.0	0.20	0.95	0.77
5.0	8.58	0.61	0.14	0.50	0.62	1.0	0.12	0.92	0.80
7.0	12.22	0.63	0.10	0.50	0.68	1.0	0.08	0.89	0.82
9.0	15.89	0.63	0.08	0.51	0.72	1.0	0.06	0.87	0.83
11.0	19.56	0.62	0.06	0.51	0.75	1.0	0.05	0.85	0.84
				Water					
10.0	6.38	0.42	0.16	1.0	0.86	1.0	0.12	0.43	0.93
15.0	9.67	0.48	0.10	1.0	0.87	1.0	0.10	0.48	0.95
20.0	12.97	0.51	0.08	1.0	0.87	1.0	0.08	0.50	0.96
				H_2SO_4					
0.2	0.32	0.05	0.17	0.01	0.02	1.0	3.09	1.0	0.70
0.4	0.36	0.06	0.19	0.04	0.10	1.0	2.76	1.0	0.74
0.6	0.51	0.10	0.21	0.11	0.19	1.0	1.96	1.0	0.73
0.8	0.71	0.14	0.24	0.17	0.27	1.0	1.42	1.0	0.73
1.0	0.93	0.19	0.26	0.22	0.33	1.0	1.08	1.0	0.73

The parameters of aerosol components of the volcanic cloud presented in Table 1 provide a clear pattern of the contribution of each component to the total estimate of mass concentration. It may be noted that for identical (in terms of optical parameters) volcanic rocks andesite and basalt, the difference in the mass concentration can reach 10% at $r_{\text{ef}} = 3$ m. Since volcanic ash clouds in real conditions consist of the mix of various aerosol components, the mass concentration of ash in the mixtures differs significantly. Therefore, the information about the aerosol composition of the volcanic cloud is one of the main factors affecting the accuracy of retrieving mass characteristics of volcanic ash.

The dependences of r_{ef} on $_{\text{theo}}$ are constructed using (5) for each model and are used to compute approximation functions. In the present study, such dependences were constructed for the spectral characteristics of the Meteosat-9 SEVIRI imager channels. Figure 1 presents the example of the dependences of r_{ef} on $_{\text{theo}}$ for some volcanic cloud models.

The approximation of points on the graph is carried out by the fifth-order polynomial like

$$\ln(y) \quad c_5x^5 \quad c_4x^4 \quad c_3x^3 \quad c_2x^2 \quad c_1x \quad c_0 \tag{9}$$

where x is the variable; c_i is coefficients.

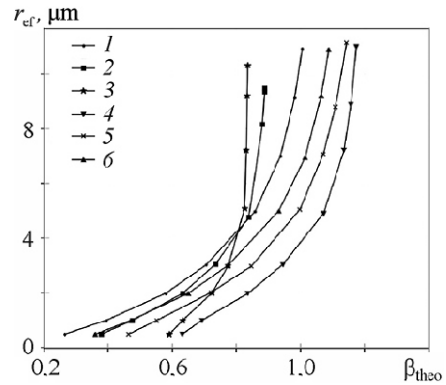

Fig. 1. The dependence of effective radius r_{ef} on the coefficient $_{theo}$ for different models of volcanic clouds. (*1*) Andesite (100%); (*2*) andesite (70%)/H_2SO_4 (30%); (*3*) andesite (30%)/H_2SO_4 (70%); (*4*) andesite (30%)/water (70%); (*5*) andesite (50%)/water (50%); (*6*) andesite (70%)/water (30%).

As the functions of spectral sensitivity of the channels for various satellite instruments can differ from each other, the program code available at https://www.dvrcpod.ru/ASH.php was created for convenience of calculating the coefficients in (9).

Figure 1 shows that the highest sensitivity to r_{ef}, as a rule, is observed in the range of r_{ef} = 0.5–6 m (i.e., relatively significant changes in $_{theo}$ with a relatively small change in r_{ef}). As soon as r_{ef} reaches a certain upper threshold, a different situation is observed: a relatively small variation in $_{theo}$ leads to significant changes in r_{ef}. Thus, there are significant uncertainties in retrieving the characteristics of large ash particles. For example, it is difficult to identify the ash particles mixed with H_2SO_4 when their size exceeds 6 m (see Fig. 1), especially when the concentration of H_2SO_4 particles per unit volume is dominant. Actually, if there are large particles in the distribution, this may lead to the incorrect choice of the model and, hence, to the incorrect estimation of r_{ef} and M_{aer}.

Before retrieving the volcanic ash parameters, the pixel containing ash should be identified in the image. The reverse absorption technique was used to detect ash in satellite images [3]. The method is based on taking into account both the difference in brightness temperature at the wavelengths of 11 and 12 m and spectral brightness coefficients at the wavelengths of 0.6 and 3.7 m. This method, unlike classic approaches [23], is more sensitive to the presence of volcanic ash including that mixed with cloudiness. After detecting each ash-containing pixel, the model of optical parameters is chosen. For the model selection, the ratios of effective absorbing optical depth $_{ef}$ at the wavelengths of 12/11 and 8.5/11 m calculated using (5) and the ratio of reflection coefficients for the channels of 3.7 and 0.6 m (RAT(3.7/0.6)) measured with the satellite instrument were used. The additional use of the ratios RAT(3.7/0.6) and the ratio of $_{ef}$ for the channels of 8.5 and 11 m, according to [19, 21], allows identifying volcanic clouds against a background of common clouds. The calculations were performed over the water surface with albedo equal to 0.03 for different combinations of viewing angles and illumination with account of the impact of trace gases on radiation intensity in the satellite instrument channels. The computation was carried out using the rapid radiative transfer model based on the DISORT (Discrete Ordinates Radiative Transfer) program code [6] from the libRadtrtan library (www.libradtran.org) [15].

The minimal residual method [8] defined by the following expression is used to choose the model:

$$^{2} \quad {}_{i\ 1}^{3} \{[S_{obs,i}(\ (12, 11),\ \ (8.5, 11), \mathrm{RAT}(3.7, 0.6)) \\ S_{theo,i}(\ (12, 11),\ \ (8.5, 11), \mathrm{RAT}(3.7, 0.6))]^2\}/\ {}_{i}^{2} \tag{10}$$

where S is the vector of parameters; ^{2} is the residual; $_i$ is the standard deviation ($(S_{obs,i})$).

The sum of squared residuals ^{2} is calculated for each optical model; then, such minimum value of ^{2} is determined to which the chosen model (for which the certain approximation function exists) will correspond. The value of $_{ef}$(12/11) is used as an argument at the input of the approximation function, and r_{ef} is calculated. Then, the value of $k_{ext,11}$ is extracted from the lookup tables, and the value of M_{aer} is determined using (7).

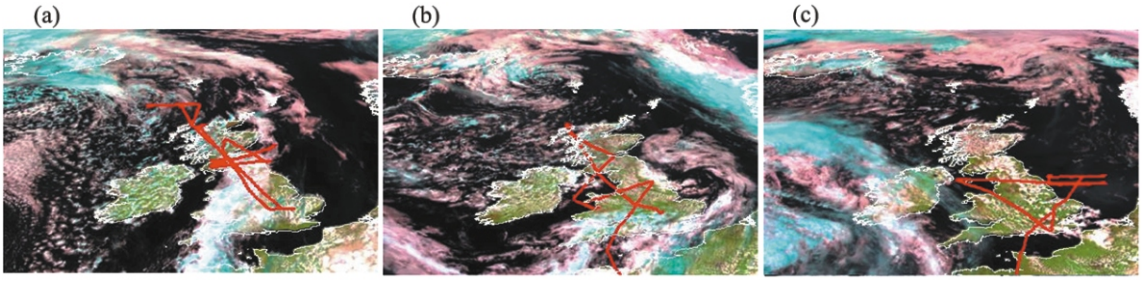

Fig. 2. The FAAM BAe-146 research aircraft trajectories combined with SEVIRI satellite images for May 2010: (a) May 14 (12:00 UTC); (b) May 16 (14:00 UTC); (c) May 17 (15:00 UTC).

ANALYSIS OF RESULTS

The Meteosat-9 SEVIRI measurements with a spatial resolution of 3 km at the subsatellite point and with the 15-minute observation interval were used to implement the above technique for retrieving cloud parameters. The data were taken from the archive https://archive.eumetsat.int. The eruption of the Eyjafjallajokull volcano (Iceland) in May 2010 was chosen as an object of research. This case is unique because ash clouds from this eruption were studied well as a result of direct ground-based [5, 10], aircraft [12, 14], and satellite measurements [13, 24].

The quality of retrieving volcanic ash parameters was assessed using the data obtained during the experimental flight of the FAAM (Facility for Airborne Atmospheric Measurements) BAe-146 research aircraft over Great Britain and surrounding seas in May 2010. More detail on this experiment is provided in [12, 14]. The measurements were performed using the onboard lidar in the near-UV region at the wavelength of 0.355 m under certain safety measures, when the cloud particle concentration did not exceed 2000 mg/m^3. The lidar has a spatial vertical resolution of 45 m and temporal horizontal resolution of 1 minute, which corresponds to the horizontal resolution along the flight direction of 7–11 km. Figure 2 presents the FAAM BAe-146 passes (the red curve) coupled with SEVIRI satellite images for May 14, 16, and 17, 2010.

The results of lidar measurements obtained during the experiment were checked for the presence of cloudiness and other aerosols, that were subsequently removed from the dataset. Based on the results of checking and processing lidar data, the vertical distributions of concentration $W_{\text{aer, lid}}$ and volumetric extinction coefficient $_{\text{ext, lid}}$ were calculated and are presented in Figs. 3 and 4. Each vertical profile corresponds to the particular time and geographic coordinates.

To proceed from the vertical distribution of $W_{\text{aer, lid}}$ and $_{\text{ext, lid}}$ to the column values, it is necessary to integrate data by height using the following expressions:

$$M_{\text{aer, lid}} \quad \int_{z_1}^{z_2} W_{\text{aer, lid}}(z)dz,$$
$$_{\text{aer, lid}} \quad \int_{z_1}^{z_2} k_{\text{ext, lid}}(z)dz \tag{11}$$

where $M_{\text{aer, lid}}$ is the mass concentration, g/m^2; $_{\text{aer, lid}}$ is the optical depth at the wavelength of 0.355 m; z_1, z_2 are the base and top of the volcanic cloud, respectively.

The following conditions were specified for integration: the base was assumed equal to 2 km, the top was 300 m below the aircraft flight height [14]. In addition, the value of $_{\text{aer}}$ for satellite data is retrieved for the wavelength of 11 m, while the lidar measured at the wavelength of 0.355 m. The following expression is used to convert $_{\text{aer}}$ to the wavelength of 0.355 m:

$$_{0.355} \quad \frac{_{11}k_{\text{ext, 0.355}}}{k_{\text{ext, 11}}(1 \quad _{11})} \tag{12}$$

where $_{0.355}$ is the optical depth at the wavelength of 0.355 m calculated from SEVIRI data.

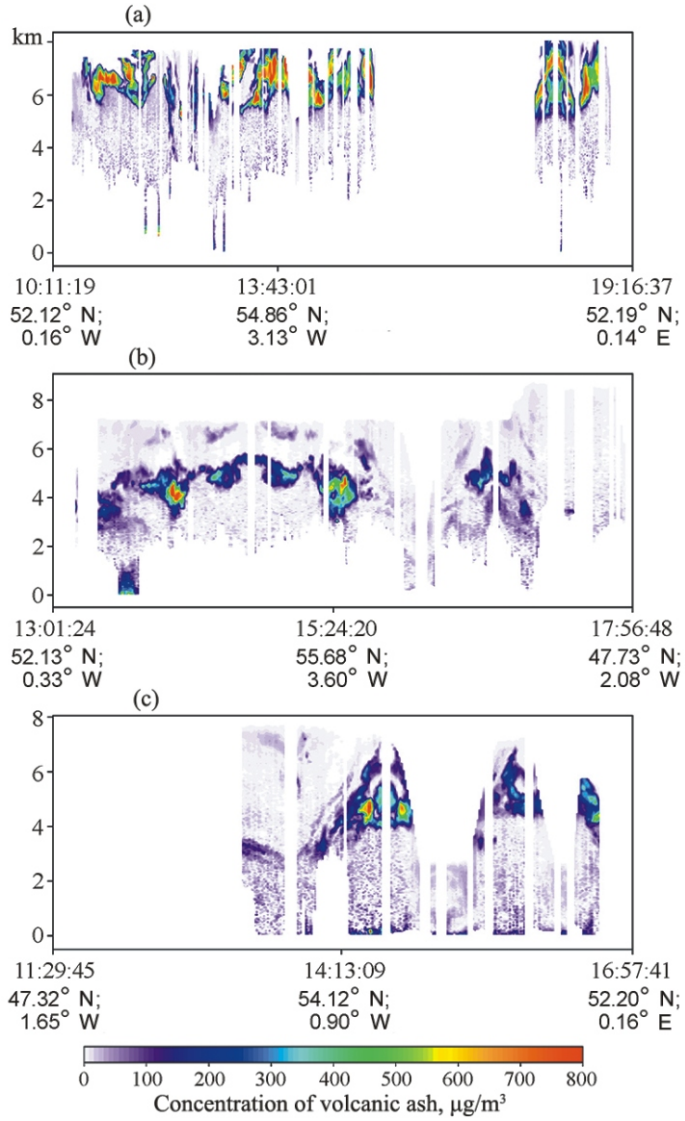

Fig. 3. The concentration of volcanic ash derived from lidar measurements during the FAAM BAe-146 research aircraft flight on May 2010: (a) May 14; (b) May 16; (c) May 17.

The comparison of satellite- and aircraft-based estimates of volcanic ash content and optical depth is carried out by the following scheme. The correction of the parallax effect (when an object is observed from the geostationary orbit at large zenith angles, its true position does not correspond to the observed one) is preliminarily carried out for each SEVIRI session. Then, the SEVIRI observation time is compared with the aircraft pass time. The data are selected when the time difference between them does not exceed 2 minutes. After that, the spatial binding is performed: the nearest aircraft measurement is searched for each pixel with ash according to SEVIRI data. The comparison takes into account the results of measurements with the ash mass concentration above 0.1 g/m^2 in order not to consider measurements with no volcanic ash. The datasets are formed separately for satellite and aircraft measurements, and their results are compared (Fig. 5).

In accordance to the conditions of the above comparison scheme, 56 cases were selected for the whole of aircraft measurements. The comparison was performed for different dates, which may indicate uniqueness of each case characterized by different particle concentration and optical depth of the volcanic cloud. Below, the results of the comparison of volcanic ash parameters are presented for each measurement day in May 2010:

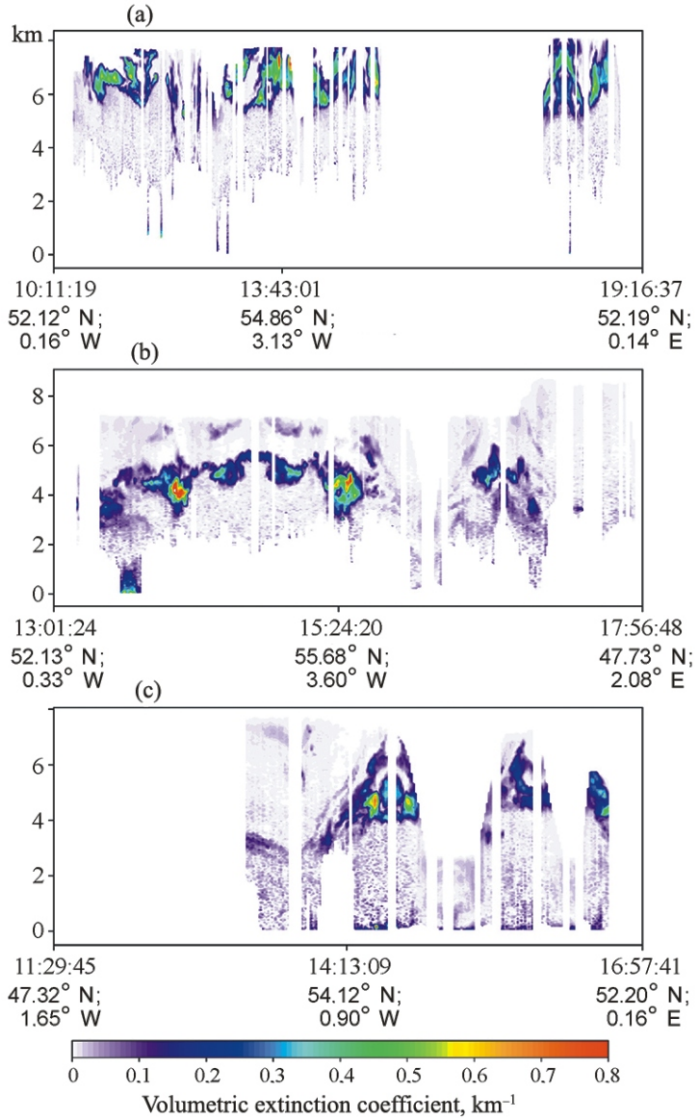

Fig. 4. The volumetric extinction coefficient for volcanic ash derived from lidar measurements during the FAAM BAe-146 research aircraft flight in May 2010: (a) May 14; (b) May 16; (c) May 17.

Date	May 14	May 16	May 17
Number of cases	42	12	2
Mass concentration			
RMSE	0.19	0.08	0.25
MAE	0.11	0.06	0.24
Optical depth			
RMSE	0.15	0.25	0.34
MAE	0.11	0.19	0.34

(RMSE is the root-mean-square error, MAE is the mean absolute error).

The coefficient of correlation between the satellite and aircraft estimates of optical depth and mass concentration of volcanic ash is more than 0.7, which indicates a high consistency of the parameters.

The ash samples were also taken during the FAAM BAe-146 research aircraft flight. The analysis revealed that particles in the atmospheric layer are lognormally distributed, with the prevalence of the 1–10 m size [12]. The distribution peak is observed for the particle size of 1.8 m. It agrees well with the SEVIRI-based

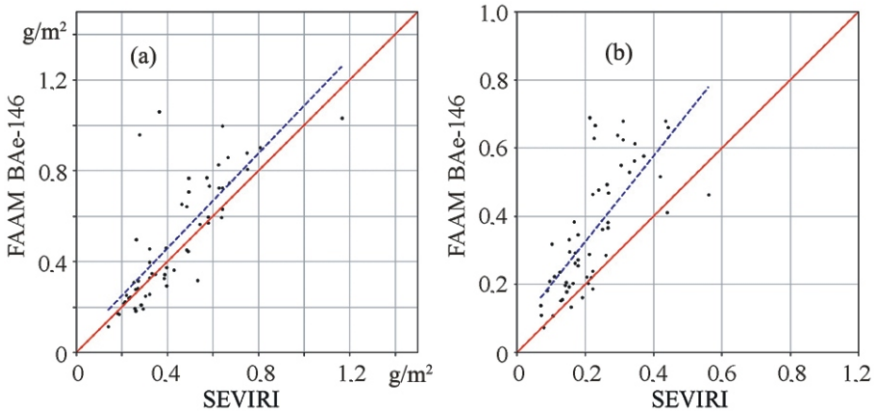

Fig. 5. The comparison of volcanic ash parameters retrieved from aircraft (FAAM BAe-146) and satellite (SEVIRI) measurements: (a) mass concentration; (b) optical depth at the wavelength of 0.355 m. The correlation coefficient $R = 0.79$ and 0.73, respectively; the root-mean-square error RMSE = 0.17 and 0.18; the mean absolute error MAE = 0.11 and 0.14; the maximum time difference between the aircraft pass and the satellite observation is 120 s.

ash particle distribution presented in Fig. 6, that was obtained for all detected ash pixels in the satellite images for the analyzed dates.

DISCUSSION OF RESULTS

Using the data of independent aircraft measurements during the Eyjafjallajokull volcano eruption allowed evaluating the volcanic ash parameters retrieved from satellite data. There is a high correlation between the satellite and aircraft estimates of volcanic ash parameters. At the same time, the mass concentration and optical depth obtained from the aircraft lidar data are always systematically higher than the satellite-retrieved ones.

There is a number of factors in which satellite estimates of volcanic ash parameters can differ from the lidar ones. The main factor is spatial resolution. The measurements of the narrow lidar beam have low spatial resolution across the survey area (about several meters) and rather high resolution (7–11 km) along it. One lidar measurement corresponds to ~8–9 pixels (~9–10 km) of the satellite measurement. One more essential factor is the difficulty of determining the ratio of the lidar backscattering coefficient to the extinction coefficient of volcanic ash. The lidar beam has a strict backscattering, and SEVIRI measurements take into account both the radiation scattering in all directions and absorption. The difference in the estimates of ash parameters is also affected by the vertically developed structure of the volcanic cloud. Since the satellite instrument measures radiation coming directly from the upper layer of the volcanic cloud, in case of multi-layer clouds it cannot receive information about the underlying layers, where ash particle concentration can be often higher than in the upper layer of the cloud. However, despite the above factors, the satellite and lidar estimates of volcanic ash parameters are in good agreement.

CONCLUSIONS

The method for retrieving the volcanic ash parameters from satellite data is presented. Its fundamental difference from the methods based on the "split transparency window" consists in the simultaneous use of different optical models of volcanic clouds in a wide range of wavelengths: from visible to infrared. The model data contain optical information not only about volcanic rocks like andesite and basalt but also about their combinations with water drops and the aqueous solution of sulfuric acid. The parameters of volcanic ash from the Eyjafjallajokull volcano eruption in May 2010 retrieved from satellite data are consistent with the similar results of aircraft measurements. The high correlation and small standard deviation indicate the efficiency of the presented technique. It should be noted that the accuracy of retrieved parameters directly depends on the choice of optical models of volcanic clouds.

The developed models and algorithms form the base for determining the parameters of the ash from volcanoes on the Kamchatka and Kuril Islands based on data of Meteor-M and Elektro-L Russian meteorological satellites jointly with measurements of foreign meteorological satellites. The obtained volcanic ash

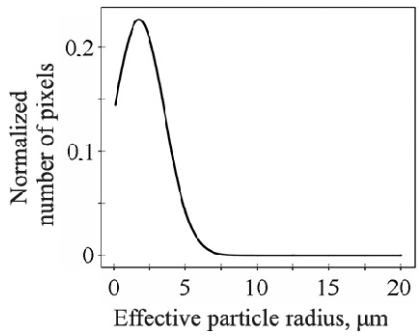

Fig. 6. The size distribution of volcanic ash particles according to SEVIRI data (for May 14, 16, and 17, 2010). $N = 295011$; $= 1.76$.

parameters will be used in the VolSatView system. It was developed by the specialists from the Institute of Volcanology and Seismology of Far Eastern Branch of Russian Academy of Sciences (FEB RAS), Space Research Institute of RAS, Computing Center of FEB RAS, and Far Eastern Branch of Planeta Research Center for Space Hydrometeorology and is intended for the comprehensive solution to the problems of the timely detection of increased volcano activity, identification and tracking of volcanic ash clouds, operational warning of the relevant services about the appearance of danger [2].

REFERENCES

1. O. A. Girina, E. A. Lupyan, A. A. Sorokin, D. V. Mel'nikov, I. M. Romanova, A. V. Kashnitskii, I. A. Uvarov, S. I. Mal'kovskii, S. P. Korolev, A. G. Manevich, and L. S. Kramareva, *Integrated Monitoring of Explosive Eruptions of the Kamchatka Volcanoes* (IViS DVO RAN, 2018) [in Russian].
2. E. I. Gordeev, O. A. Girina, E. A. Lupyan, A. A. Sorokin, L. S. Kramareva, V. Yu. Efremov, A. V. Kashnitskii, I. A. Uvarov, M. A. Burtsev, I. M. Romanova, D. V. Mel'nikov, A. G. Manevich, S. P. Korolev, and A. L. Verkhoturov, "Volsatview Information System for Solving the Problems of Volcano Activity Monitoring on the Kamchatka and Kuril Islands," Vulkanologiya i Seismologiya, No. 6 (2016) [in Russian].
3. A. A. Filei, "Automatic Detection of Volcanic Ash Using Satellite Data," Sovremennye Problemy Distantsionnogo Zondirovaniya iz Kosmosa, No. 4, **16** (2019) [in Russian].
4. A. A. Filei, "Development of Models of Optical Parameters of Volcanic Clouds for Remote Sensing of Earth from Space," Optika Atmosfery i Okeana, No. 2, **33** (2020) [in Russian].
5. A. Ansmann, M. Tesche, P. Seifert, S. Grob, V. Freudenthaler, A. Apituley, K. M. Wilson, I. Serikov, H. Linne, B. Heinold, A. Hiebsch, F. Schnell, J. Schmidt, I. Mattis, U. Wandinger, and M. Wiegner, "Ash and Fine-mode Particle Mass Profiles from EARLINET-AERONET Observations over Central Europe after the Eruptions of the Eyjafjallajokull Volcano in 2010," J. Geophys. Res.: Atmos., No. 20, **116** (2011).
6. R. Buras, T. Dowling, and C. Emde, "New Secondary-scattering Correction in DISORT with Increased Efficiency for Forward Scattering," J. Quant. Spectrosc. Radiat. Transfer, No. 12, **112** (2011).
7. S. Corradini, C. Spinetti, E. Carboni, C. Tirelli, M. F. Buongiorno, S. Pugnaghi, and G. Gangale, "Mt. Etna Tropospheric Ash Retrieval and Sensitivity Analysis Using Moderate Resolution Imaging Spectroradiometer Measurements," J. Appl. Remote Sens., No. 1, **2** (2008).
8. K. D. Costa, *Model Fitting and Error Estimation. Systems Biology: Biomedical Modeling* (2010), http://clip.med.yale.edu/courses/brdu/Costa_ODE.pdf.
9. D. S. Ensor and M. J. Pilat, "Calculation of Smoke Plume Opacity from Particulate Air Pollutant Properties," J. Air Pollut. Contr. Assoc., No. 8, **21** (1971).
10. J. Gasteiger, S. Gross, V. Freudenthaler, and M. Wiegner, "Volcanic Ash from Iceland over Munich: Mass Concentration Retrieved from Ground-based Remote Sensing Measurements," Atmos. Chem. Phys., **11** (2011).
11. T. Inoue, "On the Temperature and Effective Emissivity Determination of Semi-transparent Cirrus Clouds by Bispectral Measurements in the 10 Micron Window Region," J. Meteorol. Soc. Japan, **63** (1985).
12. B. Johnson, K. Turnbull, P. Brown, R. Burgess, J. Dorsey, A. J. Baran, H. Webster, J. Haywood, R. Cotton, Z. Ulanowski, E. Hesse, A. Woolley, and P. Rosenberg, "In Situ Observations of Volcanic Ash Clouds from the FAAM Aircraft during the Eruption of Eyjafjallajokull in 2010," J. Geophys. Res.: Atmos., No. 20, **117** (2012).
13. S. Newman, L. Clarisse, D. Hurtmans, F. Marenco, B. Johnson, K. Turnbull, S. Havemann, A. J. Baran, D. O'Sullivan, and J. M. Haywood, "A Case Study of Observations of Volcanic Ash from the Eyjafjallajokull Eruption: 2. Airborne and Satellite Radiative Measurements," J. Geophys. Res.: Atmos., No. 20, **117** (2012).

14. F. Marenco, B. Johnson, K. Turnbull, S. Newman, J. Haywood, H. Webster, and H. Ricketts, "Airborne Lidar Observations of the 2010 Eyjafjallajokull Volcanic Ash Plume," J. Geophys. Res.: Atmos., No. 20, **116** (2011).
15. B. Mayer, A. Kylling, C. Emde, R. Buras, U. Hamann, J. Gasteiger, and B. Richter, *LibRadtran User's Guide* (2017), http://www.libradtran.org/doc/libRadtran.pdf.
16. M. P. Mccormick, L. W. Thomason, and C. R. Trepte, "Atmospheric Effects of the Mt Pinatubo Eruption," Nature, No. 6513, **373** (1995).
17. *Oxford Economics. The Economic Impacts of Air Travel Restrictions Due to Volcanic Ash* (2010), http://www.oxfordeconomics.com/publication/open/240242.
18. F. Parol, J. C. Buriez, G. Brogniez, and Y. Fouquart, "Information-content of AVHRR Channels 4 and 5 with Respect to the Effective Radius of Cirrus Cloud Particles," J. Appl. Meteorol., **30** (1991).
19. M. Pavolonis, "A Daytime Complement to the Reverse Absorption Technique for Improved Automated Detection of Volcanic Ash," J. Atmos. Ocean. Technol., **23** (2006).
20. M. Pavolonis, "Advances in Extracting Cloud Composition Information from Spaceborne Infrared Radiances—A Robust Alternative to Brightness Temperatures. Part I: Theory," J. Appl. Meteorol. Climatol., No. 9, **49** (2010).
21. M. Pavolonis, A. K. Heidinger, and J. Sieglaff, "Automated Retrievals of Volcanic Ash and Dust Cloud Properties from Upwelling Infrared Measurements," J. Geophys. Res.: Atmos., No. 3, **118** (2013).
22. M. J. Pilat and D. S. Ensor, "Comparison between the Light Extinction Aerosol Mass Concentration Relationship of Atmospheric and Air Pollutant Emission Aerosols," Atmos. Environ., **5** (1971).
23. A. J. Prata, "Observations of Volcanic Ash Clouds in the 10–12-micron Window Using AVHRR/2 Data," Int. J. Remote Sens., No. 4–5, **10** (1989).
24. A. J. Prata and A. T. Prata, "Eyjafjallajokull Volcanic Ash Concentrations Determined Using Spin Enhanced Visible and Infrared Imager Measurements," J. Geophys. Res.: Atmos., No. 20, **117** (2012).
25. P. C. Reid and R. E. Hari, "Global Impacts of the 1980s Regime Shift," Glob. Change Biol., **22** (2016).
26. H. C. van de Hulst, *Light Scattering by Small Particles*, Vol. 1 (Dover Publication, 1981).
27. S. Wen and W. I. Rose, "Retrieval of Sizes and Total Mass of Particles in Volcanic Clouds Using AVHRR Bands 4 and 5," J. Geophys. Res.: Atmos., **99** (1994).
28. *WMO SCOPE-Nowcasting. Meeting on the Intercomparison of Satellite-based Volcanic Ash Retrieval Algorithms Final Report* (2015), http://www.wmo.int/pages/prog/sat/documents/SCOPE-NWCPP2_VAIntercompWSReport2015.pdf.